

GAMMA-RAY BURST EARLY OPTICAL AFTERGLOW: IMPLICATIONS FOR THE INITIAL LORENTZ FACTOR AND THE CENTRAL ENGINE

BING ZHANG¹, SHIHO KOBAYASHI^{1,2}, & PETER MÉSZÁROS^{1,2}

¹Department of Astronomy & Astrophysics, Pennsylvania State University, University Park, PA 16802

²Department of Physics, Pennsylvania State University, University Park, PA 16802

Draft version May 22, 2019

ABSTRACT

Early optical afterglows have been observed from GRB 990123, GRB 021004, and GRB 021211, which reveal rich emission features attributed to reverse shocks. It is expected that *Swift* will discover many early afterglows. Here we introduce a straightforward recipe for directly constraining the initial Lorentz factor of the fireball using the combined forward and reverse shock optical afterglow data. The scheme is largely independent of the shock microphysics. We identify two types of combinations of the reverse and forward shock emission, and explore their parameter regimes. We also discuss a possible diagnostic for magnetized ejecta.

Subject headings: gamma rays: bursts - shock waves

1. INTRODUCTION

The standard Gamma-ray burst (GRB) afterglow model (Mészáros & Rees 1997a; Sari, Piran & Narayan 1998) invokes synchrotron emission of electrons from the forward external shock, and has been proven successful in interpreting the late time broadband afterglows. At these late times the fireball is already decelerated and has entered a self-similar regime, in which precious information about the early ultra-relativistic phase is lost. In the very early afterglow epoch, the emission from the reverse shock propagating into the fireball itself also plays a noticeable role, especially in the low frequency bands, e.g. optical or radio (Mészáros & Rees 1997a; Sari & Piran 1999b), and information about the fireball initial Lorentz factor could in principle be retrieved from the reverse shock data. For a long time, evidence for reverse shock emission was available only from GRB 990123 (Akerlof et al. 1999; Sari & Piran 1999a; Mészáros & Rees 1999; Kobayashi & Sari 2000). Recently, thanks to prompt localizations of GRBs by the *High Energy Transient Explorer 2* (*HETE-2*) (e.g. Shirasaki et al. 2002; Crew et al. 2002) and rapid follow-ups by robotic optical telescopes (e.g. Fox 2002; Li et al. 2002; Fox & Price 2002), reverse shock emission has also been identified from GRB 021004 (Kobayashi & Zhang 2003) and GRB 021211 (Fox et al. 2003; Li et al. 2003; Wei 2003). It is expected that the *Swift* mission will record many GRB early optical afterglows after its launch scheduled in December 2003, which will unveil a rich phenomenology of both reverse and forward shock emission.

Here we propose a paradigm to analyze the early optical afterglow data, starting from tens of seconds after the gamma-ray trigger. By combining the emission information from both the forward and the reverse shocks, we discuss a way to derive or constrain the initial Lorentz factor of the fireball directly from the observables. The method does not depend on the poorly-known shock microphysics (e.g. the equipartition parameters ϵ_e and ϵ_B). We also categorize the early optical afterglows into two types and discuss the parameter regimes for both cases.

2. FORWARD AND REVERSE SHOCK COMPARISON

We consider a relativistic shell (fireball ejecta) with an isotropic equivalent energy E and an initial Lorentz factor η expanding into a homogeneous interstellar medium with particle number density n at a redshift z . In the observer's frame, one can define a timescale when the accumulated ISM mass is $1/\eta$ of the ejecta mass, i.e., $t_\eta = [(3E/4\pi\eta^2 nm_p c^2)^{1/3}/2\eta^2 c](1+z)$. This is the fireball deceleration time if the burst duration $T < t_\eta$. For $T > t_\eta$, the deceleration time is delayed to T . The critical condition $T = t_\eta$ defines a critical initial Lorentz factor

$$\eta_c \simeq 125 E_{52}^{1/8} n^{-1/8} T_2^{-3/8} [(1+z)/2]^{3/8}, \quad (1)$$

where the convention $Q = 10^n Q_n$ is used. Notice that η_c depends on E , T , z , and n (eq.[1]). The former three are readily measurable by *Swift*. The ISM density n can be measured in most cases with broadband fits (Panaitescu & Kumar 2001), and η_c is only weakly dependent on both n and E . Thus, η_c is essentially an observable in an idealized observational campaign. Denoting $\kappa \equiv \eta/\eta_c \equiv (T/t_\eta)^{3/8}$, one can define $\kappa > 1$ and $\kappa < 1$ as the thick and thin shell cases, respectively. When the reverse shock crosses the shell, the observer time and the ejecta Lorentz factor are (Sari & Piran 1995; Kobayashi, Piran & Sari 1999)

$$t_x = \max(t_\eta, T), \gamma_x = \min(\eta, \eta_c). \quad (2)$$

The forward shock synchrotron spectrum can be approximated as a four-segment power-law with breaks at the cooling frequency ν_c , typical frequency ν_m and the self-absorption frequency ν_a (Sari et al. 1998), and so is the reverse shock emission spectrum at $t < t_x$. For $t > t_x$, there is essentially no emission above ν_c for the reverse shock emission. For both shocks, the typical frequency, cooling frequency and the peak flux scale as $\nu_m \propto \gamma B \gamma_e^2$, $\nu_c \propto \gamma^{-1} B^{-3} t^{-2}$, and $F_{\nu, m} \propto \gamma B N_e$, where γ is the bulk Lorentz boost, B is the comoving magnetic field, γ_e is the typical electron Lorentz factor in the shock-heated region, and N_e is the total number of emitting electrons. At the crossing time, one has the relations (Kobayashi & Zhang

2003, but with a b dependence added here)

$$\frac{\nu_{m,r}(t_\times)}{\nu_{m,f}(t_\times)} \sim \hat{\eta}^{-2} b \quad (3)$$

$$\frac{\nu_{c,r}(t_\times)}{\nu_{c,f}(t_\times)} \sim b^{-3}, \quad (4)$$

$$\frac{F_{\nu,m,r}(t_\times)}{F_{\nu,m,f}(t_\times)} \sim \hat{\eta} b \quad (5)$$

where $\hat{\eta} \equiv \gamma_\times^2 / \eta \leq \eta_c$, and $b \equiv B_r / B_f$, and the subscripts ‘f’ and ‘r’ indicate forward and reverse shock, respectively. In some central engine models (e.g. Usov 1992; Mészáros & Rees 1997b), the fireball wind may be endowed with “primordial” magnetic fields, so that in principle B_r could be higher than B_f , and we have included the b parameter in a more general discussion. The forward shock emission is likely to be in the “fast cooling” regime ($\nu_{c,f} < \nu_{m,f}$) initially and in the “slow cooling” regime ($\nu_{c,f} > \nu_{m,f}$) at later times (Sari et al. 1998). For the reverse shock emission, it can be deduced from eqs. (3, 4) and eq.(11) of Sari et al. (1998) that slow cooling ($\nu_{c,r} > \nu_{m,r}$) is generally valid as long as b is not much greater than unity.

The lightcurves can be derived by specifying the temporal evolution of ν_m , ν_c , and $F_{\nu,m}$. To first order, in the forward shock (Mészáros & Rees 1997a) we have

$$\nu_{m,f} \propto t^{-3/2}, F_{\nu,m,f} \propto t^0 \quad (6)$$

while in the reverse shock for $t > t_\times$ (Kobayashi 2000, hereafter K00) we have

$$\nu_{m,r} \propto t^{-3/2}, F_{\nu,m,r} \propto t^{-1} \quad (7)$$

The optical-band lightcurve for the forward shock is well-described by the “low-frequency” case of Sari et al. (1998, their Fig.2b), characterized by a turnover of the temporal indices from $1/2$ to $3(1-p)/4$ (where p is the power-law index of the electron distribution) at the peak time $t_{p,f}$ (at which ν_m crosses the optical band, e.g. ν_R). The optical lightcurve for the reverse shock emission is more complicated, depending on whether the shell is thin or thick, whether it is in the slow or fast cooling regime, and how ν_R compares with $\nu_{m,r}(t_\times)$ and $\nu_{c,r}(t_\times)$ (see K00 for a complete discussion). For reasonable parameters, however, the cases of $\nu_R > \nu_{c,r}$ and $\nu_R < \nu_{a,r}$ are unlikely, and even if these conditions are satisfied, they do not produce interesting reverse shock signatures. Defining

$$\zeta \equiv \frac{\nu_R}{\nu_{m,r}(t_\times)}, \quad (8)$$

and specifying the slow-cooling case (which is reasonable for a large sector of parameter regimes, K00), the reverse shock lightcurves are then categorized into four specific cases with various temporal indices (α_r ’s) separated by various break times (t_b ’s), which correspond to the thick and thin solid lines in Fig.2a and Fig.3a of K00.

- (i) $\zeta > 1, \kappa < 1$: $\alpha_r \sim (5, -2)$, $t_b = t_\times$;
- (ii) $\zeta > 1, \kappa > 1$: $\alpha_r \sim (1/2, -2)$, $t_b = t_\times$;
- (iii) $\zeta < 1, \kappa < 1$: $\alpha_r \sim (5, -1/2, -2)$, $t_b = (t_{m,r,-}, t_{m,r,+})$;
- (iv) $\zeta < 1, \kappa > 1$: $\alpha_r \sim (1/2, -1/2, -2)$, $t_b = (t_\times, t_{m,r,+})$.

Here $t_{m,r,-} = \zeta^{1/6} t_\times$ and $t_{m,r,+} = \zeta^{-2/3} t_\times$ are the critical

times when $\nu_{m,r} = \nu_R$ for $t < t_\times$ and $t > t_\times$, respectively (K00). In any case, we define the final reverse shock lightcurve as $F_{\nu,r} \propto t^{-\alpha}$, where

$$\alpha = (3p + 1)/4, \quad (9)$$

which is ~ 2 for typical p values. Going backwards in time, the well-known $F_{\nu,r} \propto t^{-2}$ reverse shock lightcurve ends at t_\times for $\zeta > 1$ (with a rising lightcurve before that), but at $t = t_{m,r,+}$ for $\zeta < 1$ (with a flatter declining lightcurve, $F_{\nu,r} \propto t^{-1/2}$, before) (Fig.1).

We define as $t_{p,r}$ the time when the $F_{\nu,r} \propto t^{-2}$ lightcurve starts (which is equal to t_\times for $\zeta > 1$, and equal to $t_{m,r,+}$ for $\zeta < 1$), and define the corresponding reverse shock spectral flux as $F_{\nu,p,r}$. For the forward shock emission, it is natural to define $F_{\nu,p,f} = F_{\nu,m,f}$ at $t_{p,f}$ (Fig.1). For practical purposes, it is illustrative to derive the ratio of the two peak times and that of the two peak fluxes by making use of eqs. (3), (5), (6), (7) and (9), i.e.

$$f_t \equiv \frac{t_{p,f}}{t_{p,r}} = \begin{cases} \hat{\eta}^{4/3} b^{-2/3} \zeta^{-2/3}, & \zeta > 1, \\ \hat{\eta}^{4/3} b^{-2/3}, & \zeta < 1, \end{cases} \quad (10)$$

$$f_F \equiv \frac{F_{\nu,p,r}}{F_{\nu,p,f}} = \begin{cases} \hat{\eta} b \zeta^{-2(\alpha-1)/3}, & \zeta > 1, \\ \hat{\eta} b \zeta^{2/3}, & \zeta < 1. \end{cases} \quad (11)$$

Notice that we have intentionally defined both f_t and f_F to be (usually) larger than unity. It is interesting to observe that these forward-to-reverse relative emission ratios depend on only two unknown parameters $\hat{\eta}$ and ζ , if b is conventionally taken as unity or as a fixed fraction. Also, these equations are valid regardless of whether the shell is thin or thick (i.e. independent of κ).

3. A RECIPE TO CONSTRAIN INITIAL LORENTZ FACTOR

Reverse shock emission data have been used to estimate the initial Lorentz factor of GRB 990123 (Sari & Piran 1999a; Kobayashi & Sari 2000; Wang, Dai & Lu 2000; Soderberg & Ramirez-Ruiz 2002), but poorly-known shock microphysics parameters (e.g., ϵ_e , ϵ_B) were used in these methods. Here we introduce a simple method to do so by invoking the ratios of the forward and reverse shock emission data, for which in a first approximation the shock microphysics parameters cancel out.

Suppose that *Swift* or a similar facility detects and monitors an optical lightcurve, starting shortly after the trigger. Generally, as long as the rising portion of reverse shock lightcurve ($\propto t^5$ for thin, and $\propto t^{1/2}$ for thick shell) is detected, one can measure t_\times (except for the case iii above), and derive (Sari & Piran 1999b)

$$\eta \geq \gamma_\times = \eta_c (T/t_\times)^{3/8}, \quad (12)$$

which gives the value (or a lower limit) of η for the thin or thick shell case, respectively. Below we introduce another four-step approach to independently constrain η from the optical lightcurve alone, regardless of whether or not t_\times is identified.

Step 1: Identify (or determine limits on) the reverse shock “peak”. This “peak” is the starting point of the $\propto t^{-2}$ lightcurve, which is not necessarily the real peak. There are two cases (Fig.1). If $\zeta > 1$, the peak is identified at the transition point from the $\propto t^5$ ($\kappa < 1$) or $\propto t^{1/2}$ ($\kappa > 1$) lightcurve to the $\propto t^{-2}$ lightcurve. If $\zeta < 1$,

the “peak” is identified at the transition point from the $\propto t^{-1/2}$ to the $\propto t^{-2}$ lightcurve. It is also possible that no lightcurve break is identified. In this case, we just record the very first data point in the $\propto t^{-2}$ lightcurve. In any case, we can identify ($\bar{t}_{p,r} \geq t_{p,r}, \bar{F}_{\nu,p,r} \leq F_{\nu,p,r}$). Hereafter equalities apply for the case of precise peak identifications, while the inequalities apply for the case that only peak limits are available.

Step 2: Identify the forward shock peak. This peak is the real peak of the forward shock lightcurve, corresponding to the time when $\nu_{m,f}$ crosses the observing band. This usually occurs \sim hours after the burst trigger. Since this peak information is essential for the discussion presented here, we strongly recommend that the *Swift UVOT* instrument closely follow a GRB early lightcurve until this peak is identified (we discuss in §4 that chances are small that such a peak is buried under the reverse shock emission). When this peak is identified, we then define

$$\bar{f}_t \equiv \frac{t_{p,f}}{t_{p,r}} \leq f_t, \quad \bar{f}_F \equiv \frac{\bar{F}_{\nu,p,r}}{F_{\nu,p,f}} \leq f_F. \quad (13)$$

Step 3: Derive or constrain $\hat{\eta}$, ζ and check for consistency. Using eqs. (9), (10), (11), (13), and $\bar{f}_F/f_F = (\bar{f}_t/f_t)^\alpha$ (as derived from $F_{\nu,r} \propto t^{-\alpha}$), one can solve for ($\hat{\eta}, \zeta$) for two regimes. For $\zeta > 1$,

$$\hat{\eta} = \hat{\eta}_0 \left(\frac{\bar{f}_t}{f_t} \right)^{\frac{3}{4\alpha-7}} \leq \hat{\eta}_0, \quad \hat{\eta}_0 = \left(\frac{\bar{f}_t^{(\alpha-1)} b^{(2\alpha+1)/3}}{\bar{f}_F} \right)^{\frac{3}{4\alpha-7}} \quad (14)$$

$$\zeta = \zeta_0 \left(\frac{\bar{f}_t}{f_t} \right)^{\frac{3(4\alpha-3)}{2(4\alpha-7)}} \leq \zeta_0, \quad \zeta_0 = \left(\frac{\bar{f}_t^{3/2} b^3}{\bar{f}_F^2} \right)^{\frac{3}{4\alpha-7}}, \quad (15)$$

and for $\zeta < 1$,

$$\hat{\eta} = \hat{\eta}_0 \left(\frac{f_t}{\bar{f}_t} \right)^{3/4} \geq \hat{\eta}_0, \quad \hat{\eta}_0 = \bar{f}_t^{3/4} b^{1/2}, \quad (16)$$

$$\zeta = \zeta_0 \left(\frac{f_t}{\bar{f}_t} \right)^{\frac{12\alpha-9}{8}} \geq \zeta_0, \quad \zeta_0 = \left(\frac{\bar{f}_t^{3/2} b^3}{\bar{f}_F^2} \right)^{-3/4}. \quad (17)$$

In the above, both $\hat{\eta}_0$ and ζ_0 can be always directly measured from the lightcurves (derived from \bar{f}_F , \bar{f}_t , and α), and the real ($\hat{\eta}, \zeta$) values should be corrected with a parameter involving some powers of (\bar{f}_t/f_t) . When $t_{p,r}$ is identified, this correction is unity, and one can also immediately determine whether $\zeta > 1$ or $\zeta < 1$ from the early lightcurves (Fig.1). Otherwise, (\bar{f}_t/f_t) could be constrained from the lightcurve, and one can derive a range of $\hat{\eta}$ for both $\zeta > 1$ and $\zeta < 1$. Both solutions are possible and one needs additional information (e.g. peak time of the radio flare) to break the degeneracy.

Step 4: Derive η from $\hat{\eta}$ and check with κ . According to the definition of $\hat{\eta}$, one has

$$\eta = \begin{cases} \hat{\eta}, & \kappa < 1, \\ \eta_c^2/\hat{\eta}, & \kappa > 1, \end{cases} \quad (18)$$

With the value or range of $\hat{\eta}$ derived in step 3, one can derive the value or range of η . If the information about the κ

can be inferred (e.g. from the slope of the rising lightcurve or by comparing t_\times with T if both are measured), the η value can be eventually identified or further constrained.

We note two caveats about our method. First, it involves a value of b (the reverse to forward comoving magnetic field ratio), so one cannot determine η without specifying b . The usual standard assumption is that $b = 1$. However, when independent information about η is available (e.g. GRB 990123), constraints on b may be obtained (§5). Second, the radiative loss correction in the early forward shock evolution may be significant. This gives a correction factor of $\sim (t_{p,f}/t_\times)^{(17/16)\epsilon_e}$ (Sari 1997) to $F_{\nu,p,f}$. When doing case studies, this should be taken into account.

4. CLASSIFICATION OF EARLY OPTICAL AFTERGLOWS

Regardless of the variety of early lightcurves, the reverse shock $F_{\nu,r} \propto t^{-\alpha}$ emission component is expected to eventually join with the forward shock emission lightcurve. We can identify two cases (Fig.1). *Type I (Rebrightening):* The reverse shock component meets the forward shock component before the forward shock peak time, as observed in GRB 021004 (Kobayashi & Zhang 2003). *Type II (Flattening):* The reverse shock component meets the forward shock component after the forward shock peak time. GRB 021211 may be a marginal case example (Fox et al. 2003; Li et al. 2003; Wei 2003).

The condition for a flattening type is $F_{\nu,r}(t_{p,f}) > F_{\nu,p,f}$. Using eqs.(10) and (11), noticing $F_{\nu,r} \propto t^{-\alpha}$, the flattening or type-II condition turns out to be

$$\hat{\eta} < b^{\frac{2\alpha+3}{4\alpha-3}} \zeta^{\frac{2}{4\alpha-7}} \quad (19)$$

for both $\zeta > 1$ and $\zeta < 1$. We can see that the type II condition is very stringent, especially when b is small. We expect that rebrightening lightcurves should be the common situation. When a flattening lightcurve is observed, most likely one has $\zeta \gg 1$, i.e, the peak frequency for the reverse shock emission is well below the optical band. This should usually involve very low luminosities in both the reverse and forward shock emission. This may be the case of GRB 021211, which could have been categorized as an “optically dark” burst if the early reverse shock emission had not been caught. Alternatively, a flattening case may be associated with a strongly magnetized central engine, since a higher b can significantly ease the type II condition.

Using eqs.(2), (3), (8), and eq.(1) of Kobayashi & Zhang (2003), we can derive $\zeta \sim 500b^{-1}\eta_2^{-2}n^{-1/2}\epsilon_{B,-2}^{-1/2}\epsilon_{e,-1}^{-2}[g/(1/3)]^{-2}[(1+z)/2]$, where $g = (p-2)/(p-1)$. We can see that generally $\zeta > 1$, but the $\zeta \lesssim 1$ case is also allowed for some extreme parameters, which may be accompanied with bright optical flashes (e.g. GRB 990123).

5. CASE STUDIES

1. GRB 990123: The basic parameters of this burst include¹ (e.g. Kobayashi & Sari 2000 and references therein) $E_{52} \sim 140$, $z = 1.6$, $T_2 \sim 0.63$, $\alpha \sim 2$. There is a debate about n for this burst (Panaitescu & Kumar 2001; Frail et al. 2001), and we adopt a typical value $n \sim 1$. This gives $\eta_c \sim 305$. The reverse shock peak was

¹Hereafter we assume that the kinetic energy of the fireball in the deceleration phase is comparable to the energy released in gamma-rays in the prompt phase.

well determined: $(t_{p,r}, F_{\nu,p,r}) \sim (50\text{s}, 1\text{Jy})$. The lightcurve shows $\zeta \geq 1$. Since $t_{p,r} \sim T$, this is a marginal case, and $\eta \sim \eta_c \sim 300$. Unfortunately, the forward shock peak was not caught. Assuming $t_{p,f} \sim 0.1 \text{ d}$, one has $f_t \sim 170$, and $f_F \sim 5000$. The radiative correction factor is ~ 2 by adopting $\epsilon_e \sim 0.13$ (Panaitescu & Kumar 2001). With this correction, one has $\hat{\eta} \sim (0.07b^{5/3})^3$ (eq.[14]). By requiring $\hat{\eta} \sim 300$, $b \sim 15$ is required. We conclude that GRB 990123 may be giving us the first evidence for a strongly magnetized central engine.

2. GRB 021004: The parameters of this burst are (e.g. Kobayashi & Zhang 2003 and references therein) $E_{52} \sim 5.6$, $z = 2.3$, $T_2 \sim 1$. Adopting $n \sim 1$, we have $\eta_c \sim 190$. The forward shock peak is reasonably well measured, and the reverse shock peak is constrained. One has $\bar{f}_t \sim 12$, $\bar{f}_F \sim 2$. Solving for $\hat{\eta}$ and ζ , we get $\hat{\eta} \leq 220b^5$ for $\zeta > 1$ and $p \sim 2.4$ (i.e., $\alpha \sim 2$ in the asymptotic phase), and $\hat{\eta} \geq 6.5b^{1/2}$ for $\zeta < 1$. The detailed modeling of the lightcurve suggests $\zeta > 1$, and $\eta \sim 120$ for $b \sim 1$ (Kobayashi & Zhang 2003).

3. GRB 021211: The basic parameters of this burst include $E_{52} \sim 0.6$, $z = 1.0$, $T_2 \sim 0.15$, $\alpha \sim 1.8$ (Li et al. 2003; Fox et al. 2003; and references therein), so that $\eta_c \sim 240$ for $n \sim 1$. Assuming that the forward shock peak occurs close to the flattening break (marginal type-II flattening case), we have $\bar{f}_t \sim 20$, $\bar{f}_F \sim 30$. This gives $\hat{\eta} \leq (0.4b^{1.5})^{15}$ for $\zeta > 1$ and $\hat{\eta} \geq 10b^{1/2}$ for $\zeta < 1$. In any case, b should be somewhat larger than unity, and $\hat{\eta}$ is likely not large according to (19). According to (18), η should be either very high or very low. The latter is consistent with its low luminosity as expected in some models (e.g. Zhang & Mészáros 2002a).

6. CONCLUSIONS AND IMPLICATIONS

We have discussed a clean recipe for constraining the initial Lorentz factor η of GRB fireballs by making use of the early optical afterglow data alone. Data in other bands (e.g. X-ray or radio) are not needed. The input parameters are ratios of observed emission quantities, so that poorly known model parameters related to the shock microphysics (e.g. ϵ_e , ϵ_B , etc.) largely cancel out. This approach is readily applicable in the *Swift* era when many early optical afterglows are expected to be regularly caught. By combining it with other information, this method may provide, for the first time, information about the magnetic content of the ejecta. Such information about the fireball initial Lorentz factor and about whether the central engine is strongly magnetized are helpful for the identification of the GRB prompt emission site and mechanism, which are currently uncertain (e.g. Zhang & Mészáros 2002b).

We have also classified the early optical afterglow lightcurves into two types. The rebrightening case (type-I) should be very common. The flattening case (type-II) is rare, and when detected, is likely to involve a low luminosity or a strongly magnetized central engine. There is evidence that the central engine of GRB 990123 is strongly magnetized.

This work is supported by NASA NAG5-9192 and the Pennsylvania State University Center for Gravitational Wave Physics, which is funded by NSF under cooperative agreement PHY 01-14375.

REFERENCES

Akerlof, C. W. et al. 1999, *Nature*, 398, 400
 Crew, G. et al. 2002, GCN 1734, (<http://gcn.gsfc.nasa.gov/gcn/gcn3/1734.gcn3>)
 Frail, D. A., Kulkarni, S. R., Sari, R., et al. 2001, *ApJ*, 562, L55
 Fox, D. W. 2002, GCN 1564 (<http://gcn.gsfc.nasa.gov/gcn/gcn3/1564.gcn3>)
 Fox, D. W. & Price, P. A. 2002, GCN 1731 (<http://gcn.gsfc.nasa.gov/gcn/gcn3/1731.gcn3>)
 Fox, D. W. et al. 2003, *ApJL*, in press ([astro-ph/0301377](http://arxiv.org/abs/astro-ph/0301377))
 Kobayashi, S 2000, *ApJ*, 545, 807 (K00)
 Kobayashi, S, Piran, T & Sari, R. 1999, *ApJ*, 513, 669
 Kobayashi, S, & Sari, R. 2000, *ApJ*, 542, 819
 Kobayashi, S, & Zhang, B. 2003, *ApJ*, 582, L75
 Li, W. Filippenko, A. V., Chornock, R. & Jha, S. 2002, GCN 1737 (<http://gcn.gsfc.nasa.gov/gcn/gcn3/1737.gcn3>)
 Li, W. Filippenko, A. V., Chornock, R. & Jha, S. 2003, *ApJL*, in press ([astro-ph/0302136](http://arxiv.org/abs/astro-ph/0302136))
 Mészáros, P. & Rees, M. J. 1997a, *ApJ*, 476, 231
 —. 1997b, *ApJ*, 482, L29
 —. 1999, *MNRAS*, 306, L39
 Panaitescu, A., & Kumar, P. 2001, *ApJ*, 560, L49
 Sari, R. 1997, *ApJ*, 489, L37
 Sari, R. & Piran, T. 1995, *ApJ*, 455, L143
 —. 1999a, *ApJ*, 517, L109
 —. 1999b, *ApJ*, 520, 641
 Sari, R., Piran, T. & Narayan, R. 1998, *ApJ*, 497, L17
 Shirasaki, Y. et al. 2002, GCN 1565 (<http://gcn.gsfc.nasa.gov/gcn/gcn3/1565.gcn3>)
 Soderberg, A. M., & Ramirez-Ruiz, E. 2002, *MNRAS*, 330, L24
 Usov, V. V. 1992, *Nature*, 357, 472
 Wang, X. Y., Dai, Z. G., & Lu, T. 2000, *MNRAS*, 319, 1159
 Wei, D. M. 2003, *A&A*, submitted ([astro-ph/0301345](http://arxiv.org/abs/astro-ph/0301345))
 Zhang, B. & Mészáros, P. 2002a, *ApJ*, 571, 876
 —. 2002b, *ApJ*, 581, 1236

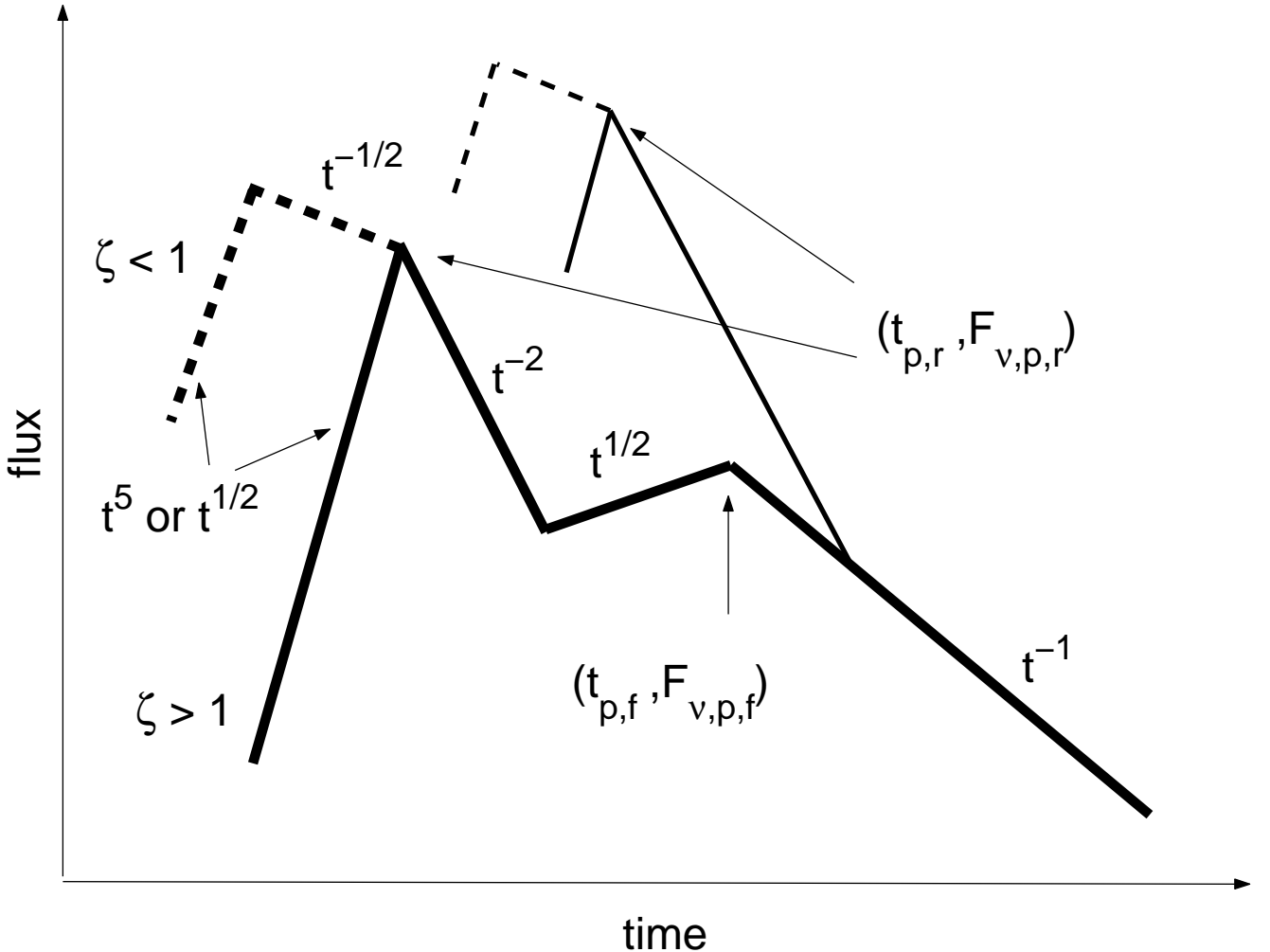


FIG. 1.— Typical lightcurves of the reverse-forward shock emission combinations. The thick lines depict a typical “rebrightening” (type I) lightcurve, while thin lines indicate a typical “flattening” (type II) lightcurve. The forward shock peak ($t_{p,f}, F_{v,m,p}$) is defined at the transition point of the $\propto t^{1/2}$ to $\propto t^{-1}$ lightcurves. The reverse shock peak ($t_{p,r}, F_{v,m,r}$) is defined at the beginning of the $\propto t^{-2}$ segment for the reverse shock emission. Before the reverse shock peak point, the lightcurve is $\propto t^{-1/2}$ for $\zeta \equiv \nu_R/\nu_{m,r}(t_X) < 1$, and is $\propto t^5$ (thin shell) or $\propto t^{1/2}$ (thick shell) for $\zeta > 1$.